Identifying Functional Flow Regimes and Fish Response for Multiple Reservoir Operating Solutions

Ana Paula Dalcin[1]; Guilherme Fernandes Marques, Ph.D.[2]; Anielly Galego de Oliveira, Ph.D.[3]; and Amaury Tilmant, Ph.D.[4]

Abstract: Flow regulation through dams increases water and energy security for society but also threatens the natural equilibrium of river basins, leaving ecosystems and communities more vulnerable. While recovering flow regime dynamics to mitigate environmental impacts is a necessary goal, its effective implementation depends on the capacity to predict the expected outcomes to multiple competing users. Although such impacts can be measured between tangible economic uses, identifying the ecological trade-offs remains a challenge. To guide the design of environmental flows and support improved ecosystem restoration, we propose a methodology framework that builds an ensemble of flow regime options based on the naturalized flow regime range variability and quantifies the ecosystem response of each option in terms of migratory fish abundance with an artificial neural network model. The flow regime options with significant responses were called functional flow regimes because they provide conditions for the recruitment success of migratory fish species, which are vulnerable to flow dynamic synchronization. Our findings indicate that functional flow regimes may still produce relevant ecological responses even without fully recovering the natural flow regime. Specific levels of magnitude, frequency, duration, and timing of a flow regime can be combined to achieve a desired level of ecological response, while there is a clear threshold above which performance gains are smaller, indicating the presence of diminishing marginal performance gains when designing environmental flows. Knowing the trade-offs of different levels of flow regime recovery gives flexibility to the negotiation process between users and managers, leading to improved reservoir operation to meet multiple competing water needs. **DOI: 10.1061/(ASCE)WR.1943-5452.0001567.**

Author keywords: Flow regime recovery; Hydropower planning; Environmental flows..

Introduction

Flow regulation through dams represents the most prevalent form of hydrological alteration of rivers with projections to expand in future decades (Grill et al. 2015; Tharme 2003). While such alteration is desirable to increase water, food, and energy security for society (Tilmant et al. 2014), the consequent disruption of flow regime patterns and reduction of aquatic and wetland habitats contribute to dramatic population declines of aquatic species (Howard et al. 2018; Palmer and Ruhi 2019). Moyle et al. (2011) estimate that more than 80% of California's native fishes are likely to be lost in the next 100 years if water management practices are not changed and the negative effects of climate change are not averted or reversed.

Because maintaining or restoring full natural flow regimes to mitigate impacts is usually unfeasible or undesirable, the concept of environmental flows has emerged to strike a balance between economic uses of water and ecosystem preservation (Poff et al. 2017). This idea explores the wide range of flow regime options that can be preserved or restored to some condition preferred by society, both in already altered rivers or where new water infrastructures are planned (Arthington et al. 2018).

Choosing between flow regime options, however, requires a capacity to predict ecological, technical, social, and economic outcomes (Arthington et al. 2018). Hydropower reservoir reoperation incorporating environmental needs often reduces generation capacity, leading to reliability and economic losses to the power sector, while water supplies may also be reduced, forcing municipalities and irrigation districts to seek out more expensive sources (Adams et al. 2017; Crespo et al. 2019). Managing such consequences remains a challenge in implementing environmental flows in a holistic perspective (Poff et al. 2017), resulting in a few examples that go beyond a minimum flow requirement (Harwood et al. 2017; Quesne et al. 2010).

Therefore, a better quantitative understanding of ecological responses to different levels of flow regime recovery is critical to also calculate the range of economic losses and engage stakeholders in decision-making. This process starts with characterizing the natural flow variability through its critical components, such as magnitude, timing, duration, frequency, and rate of change (Poff et al. 1997; Olden and Poff 2003), followed by understanding the ecological response to the natural variability and degrees of alteration

[1]Environmental Engineer, Programa de Pós-Graduação em Recursos Hídricos e Saneamento Ambiental, Instituto de Pesquisas Hidráulicas (IPH), Universidade Federal do Rio Grande do Sul (UFRGS), Porto Alegre, RS 91501-970, Brazil (corresponding author). ORCID: https://orcid.org/0000-0001-9871-7373. Email: dalcin.anap@gmail.com

[2]Associate Professor, Programa de Pós-Graduação em Recursos Hídricos e Saneamento Ambiental, Instituto de Pesquisas Hidráulicas (IPH), Universidade Federal do Rio Grande do Sul (UFRGS), Porto Alegre, RS 91501-970, Brazil. ORCID: https://orcid.org/0000-0003-0543-6279. Email: guilherme.marques@ufrgs.br

[3]Biologist, Programa de Pós-Graduação em Ecologia de Ambientes Aquáticos Continentais, Núcleo de Pesquisas em Limnologia, Ictiologia e Aquicultura (NUPÉLIA), Universidade Estadual de Maringá, Maringá, PR 87020-900, Brazil. ORCID: https://orcid.org/0000-0002-6185-1728. Email: anielly_oliveira@hotmail.com

[4]Professor, Dept. of Civil and Water Engineering, Université Laval, Quebec City, QC, Canada G1V 0A6. ORCID: https://orcid.org/0000-0001-9586-5274. Email: amaury.tilmant@gci.ulaval.ca

Note. This manuscript was submitted on May 19, 2021; approved on February 23, 2022; published online on March 30, 2022. Discussion period open until August 30, 2022; separate discussions must be submitted for individual papers. This paper is part of the ***Journal of Water Resources Planning and Management***, © ASCE, ISSN 0733-9496.

(Arthington et al. 2006), to finally calculate the trade-offs with other uses (Chen and Olden 2017; Li et al. 2020; Suen and Eheart 2006; Wild et al. 2019) and propose adaptation cost distribution among users (Marques and Tilmant 2018).

Focusing on flow regime components that trigger significant geomorphological and ecological processes (functional flow regimes) provides a strategic frame of reference to develop ecological-flow relationships and more successful recovery plans (Grantham et al. 2020; Yarnell et al. 2015). Fish are part of food web dynamics and nutrient cycling, serving as an effective indicator of ecosystem health, with the advantage of being sensitive to flow dynamic changes (Whitfield and Elliott 2002). Many studies evaluating the modification of downstream flow regimes by reservoir regulation highlight a simplification of the ichthyofauna diversity, with a marked reduction in migratory species (Cooper et al. 2017; Loures and Pompeu 2018; Pringle et al. 2000). Fisheries also represent a traditional ecosystem service provision (e.g., food and ecotourism) (Holmlund and Hammer 1999), contributing to social and economic activities.

Statistical approaches have been applied as means to quantify and interpret meaningful flow regime components that drive ecological processes to sustain fish populations and communities. Researchers like Freeman et al. (2001), Oliveira et al. (2015), Piffady et al. (2010), Tonkin et al. (2021), and Wang et al. (2019) statistically analyzed the degree of fish response to flow regime indexes, showing that the intensity, timing, and duration of flood pulses when synchronized with life stages during the spawning and recruitment processes are highly correlated with juvenile abundances. Floods trigger fish migration for spawning and connect longitudinally and laterally different habitats across floodplains, providing feeding and refuge conditions for initial growth. By retaining high flows during the rainy season to make it available during the dry season, reservoir regulation reduces or eliminates flood peaks, while higher flow periods are artificially created in the dry season. Fish recruitment is then affected.

With advances in machine learning techniques, data-driven models have also been applied to empirically model complex systems by extracting fish patterns from historical data sets. A set of environmental variables, including flow regime components, has been used to predict, for example, spatial fish occurrence (Joy and Death 2004), fish biodiversity (Hu et al. 2020), and fish recruitment probability (Fernandes et al. 2010).

Despite recent innovations, water managers still face a knowledge gap in translating the set of components of a flow regime to restore key ecological functions into objectives (McKay et al. 2012) and reservoir operating practices, as the latter need to accommodate other multiobjective demands (e.g., hydropower, irrigation, and urban supply). Fish are adapted to a certain level of flow variability, and, given the wide range of flow regime options when dealing with flow regime recovery, choosing which ones to address with reservoir operation can yield different impacts on water system reliability and expenses. Although such impacts can be measured between tangible economic uses, ecosystem response performance remains largely unknown.

This paper addresses this knowledge gap with a methodology framework that explicitly quantifies the response of different flow regime options toward a key ecosystem function to guide the formulation of environmental flows. In our paper, this function is the recruitment success of migratory fish species. The framework combines three main parts. In the first subroutine, an ensemble of flow regime options is produced based on the naturalized flow regime range variability. The second subroutine derives a set of flow metrics (indexes) to quantify the five main components (magnitude, timing, duration, frequency, and rate of change) of each flow regime option. The third subroutine contains an artificial neural network (ANN) predictive model that calculates the response of migratory young-of-the-year (YoY) fish abundance of each flow regime option using the corresponding flow regime indexes as predictors. The options with positive nonzero responses were termed functional flow regimes (or functional flows) because they provide conditions to support the recruitment success of migratory fish species. The methodology framework was applied to a study area in the Upper Paraná River Basin, a highly developed hydropower system in Brazil.

Study Area

The Upper Paraná River Basin (Fig. 1) is one of the most impounded of South America, with 65 hydropower plants and a generation installed capacity of 48,381 MW, which corresponds to about 40% of total hydropower generation in Brazil (ANA 2020b; CCEE 2020). The 230 km between Porto Primavera dam and the Itaipu reservoir is the last remaining dam-free lotic environment of the original floodplain (Oliveira et al. 2015). The reach is bounded by the operation of 56 upstream hydropower plants and 8 hydropower plants downstream of the Itaipu hydropower plant (ANA 2020b). This area still preserves some natural features for fish spawning and migration, but it also requires reservoir reoperation to recover and maintain related ecosystem services, and the trade-offs remain largely unknown.

Flooding Dynamics and Ichthyofauna Behavior

The daily level of the Paraná River is registered by the Porto São José gauging station (ID 64575003) (ANA 2020a). Flood events exclusively controlled by the Paraná River can fully cover the floodplain, connecting different habitats, such as lagoons and secondary channels (Comunello et al. 2003). Two other tributaries, the Baía and Ivinhema tributaries, affect the floodplain inundation dynamic, although they attain narrower floodplain coverage. Combined events, when Paraná River flooding occurs concomitantly with tributary flooding, are also observed.

The ichthyofauna of the Upper Paraná River is composed of 211 cataloged species divided into 2 major groups: sedentary/short-distance migratory and long-distance migratory (Ota et al. 2018). Long-distance migratory species are characterized by their larger size and longer lifespans, requiring different habitats during their life cycle for spawning, early development, and feeding (Agostinho et al. 2007). Three main movements characterize the relation between the long-distance migratory fish reproduction cycle and the flow regime in the study area (Agostinho et al. 2007; Oliveira et al. 2015).

At the beginning of the rainy season, a combined increase in the photoperiod and temperature triggers gonadal development and school formation. This is followed by an upstream migration (from October to November) when fish schools move to upstream reaches and tributaries, where eggs are laid and can develop in well-oxygenated waters with lower predation risk. High water levels (from January to March) promote the connectivity between different habitats (e.g., lagoons, channels), which enables the lateral movement of larvae along the floodplain area for feeding and refuge. The last movement occurs during decreasing water levels (from March to May) and allows backward movement toward the main river channel.

The period of low waters occurs during winter (June to September). During this phase, floodplain habitats are less connected with rivers and subject to local processes, like wind turbulence, thermal mixing, and inputs from small tributaries, which affect variations in

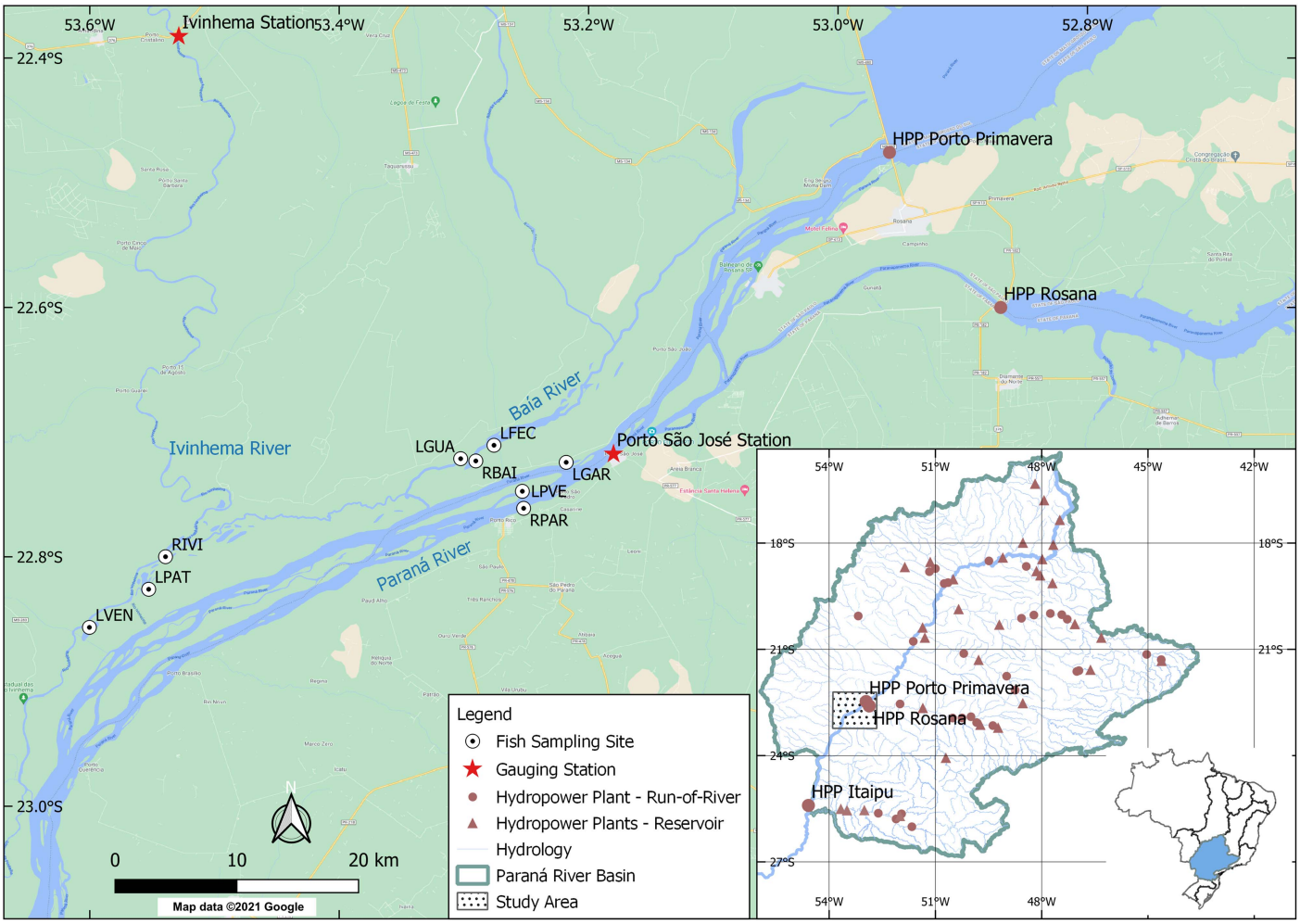

Fig. 1. Upper Paraná River floodplain, including fish sampling and flow gauging stations. (Map data © 2021 Google.)

physicochemical parameters and vegetation growth (Agostinho et al. 2000).

Fish Sampling Data

Fish sampling data span quarterly periods from March to December from 2000 to 2019 at nine sampling sites within the floodplain (Fig. 1)—three rivers (Paraná River and Ivinhema and Baía tributaries) and two adjacent lagoons for each river—as reported in Oliveira et al. (2015, 2020). The grouping of each river and its corresponding lagoons was termed a subsystem. Data from previous years were reported in Suzuki et al. (2009) with intermittent periods from 1987 to 1988 and 1992 to 1994. We chose the years 1992 to 1994, combined with the years 2000 to 2019, to build the full data set, as both periods contained available data for the same species in all fish campaigns.

Five long-distance migratory fish species were considered: *Brycon orbignyanus* (Valenciennes 1850), *Pseudoplatystoma corruscans* (Spix and Agassiz 1829), *Pterodoras granulosus* (Valenciennes 1821), *Prochilodus lineatus* (Valenciennes 1837), and *Salminus brasiliensis* (Cuvier 1816), which are the most abundant among the long-distance migratory fishes, representing almost 25% of the total number of migratory species in the Paraná River Basin. The abundance of YoY fish individuals, which represent the recruitment success of the last flood season, was determined by counting the number of individuals of given reference lengths up to 1 year old (Oliveira et al. 2020) and indexed as catch per unit effort (CPUE) (individuals/1,000 m^2 of gillnets in the course of 24 h).

The annual YoY fish abundance of each subsystem was represented as the average between the corresponding sampling sites. To represent the annual YoY fish abundance of the floodplain related to the Paraná River flow regime (Porto São José gauging station), the fish abundance average between subsystems was considered when combined flood events occurred during the rainy season. To avoid overestimating fish abundance due to tributary flooding, floodplain fish abundances were set to zero when flood events were registered only in the tributaries. Finally, for years when flood events were registered exclusively at the Paraná River, the average between subsystems considered the tributaries' abundances as zero. Fig. 6 presents the total annual YoY fish abundance for the floodplain.

Methodology

The methodology framework includes three main subroutines (Fig. 2). In the first subroutine, an ensemble of flow regime options is produced based on the naturalized flow regime range variability of the study area. The flow regime options consist of annual hydrologic time series of daily levels (covering the dry and rainy seasons that occur in an annual period). The second subroutine derives a set of flow metrics (indexes) to quantify the five main components

(magnitude, timing, duration, frequency, and rate of change) of each flow regime option. The third subroutine contains an ANN predictive model that calculates the response of migratory YoY fish abundance of each flow regime option using the set of flow regime indexes as predictors. The flow regime options with positive nonzero responses were called functional flow regimes.

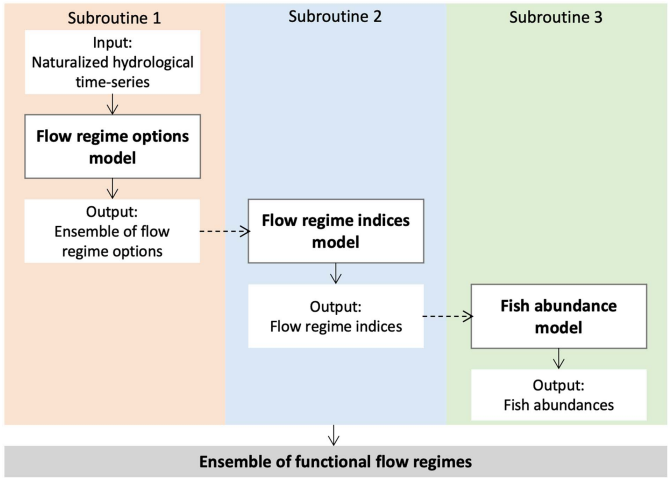

Fig. 2. Methodology framework.

Flow Regime Options Model

To generate an ensemble of flow regime options, the naturalized flow regime was first estimated by reverting the flow regulation effects and evaporation losses of the reservoirs part of the hydropower system. The resulting range of the long-term naturalized flow regime variability appears in Fig. 3, while the procedure details for its estimation are described in Appendix I.

From the naturalized flow time series, the subroutine adopts a three-step procedure: (1) the daily time series is converted to a specific time-step (e.g., biweekly or monthly) average time series and the long-term variability of the given time step is calculated (Fig. 4, left); (2) the range between the minimum and maximum values is divided into discrete states (Fig. 4, middle); and (3) combinations of sequential states are then computed (Fig. 4, right). The daily values between the monthly or biweekly time steps are then built by linear interpolation. As a result, an ensemble of annual hydrologic time series of daily level is generated representing multiple flow regime options. For example, considering a monthly time step and five discrete flow/level states results in the composition of 5^{12} different flow regime options.

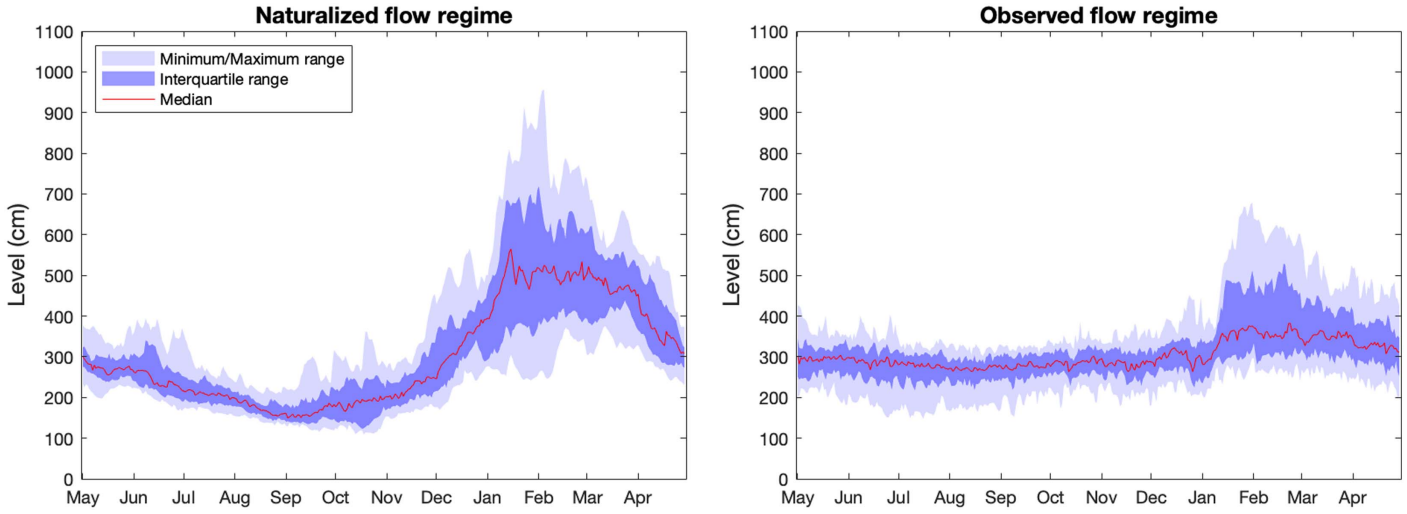

Fig. 3. Comparison of observed and naturalized flow regime at Porto São José station.

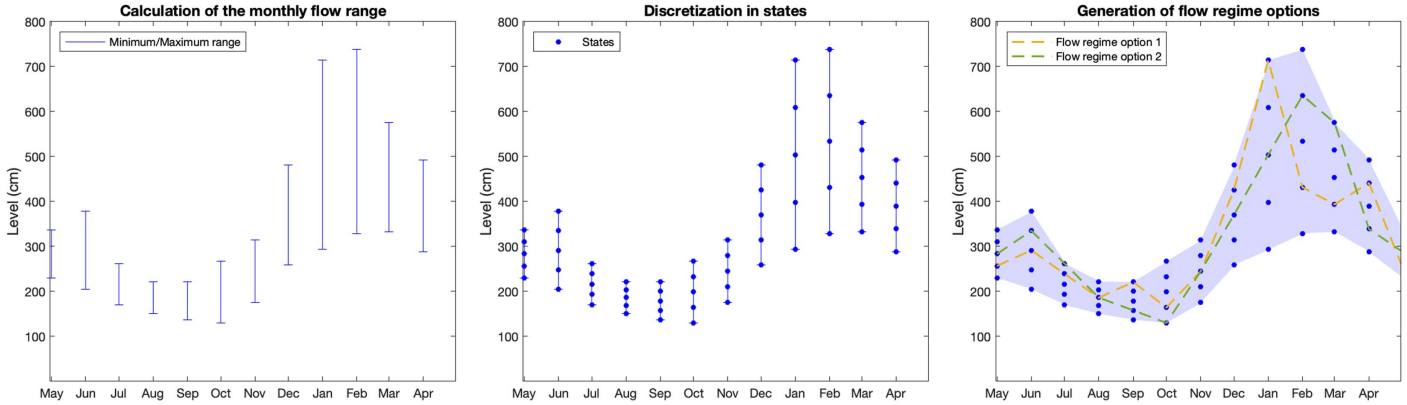

Fig. 4. Representation of generation of flow regime options.

J. Water Resour. Plann. Manage., 2022, 148(6): 04022026

Table 1. Flow regime indexes used to represent the Paraná River reach flow regime

Flow regime component	Index	Thresholds
Duration and magnitude	FSD high magnitude	Number of days where water level ≥ 610 cm during rainy season from October 1 to April 30
	FSD midmagnitude	Number of days where 540 cm ≤ water level <610 cm during rainy season from October 1 to April 30
	FSD low magnitude	Number of days where 450 cm ≤ water level <540 cm during rainy season from October 1 to April 30
	DSD	Number of days where water level ≤ 250 cm during dry season from June 1 to September 30
Magnitude	Maximum magnitude	Highest water level (cm) record during rainy season from October 1 to April 30
Timing	Flood delay	Number of days from October 1 when the first flood (water level ≥ 450 cm) was recorded
Variability (rate of change)	Flood pulses	Number of complete cycles of high (≥450 cm) and low water level during rainy season from October 1 to April 30
	Uninterrupted flood duration	Longer number of sequential days where level ≥ 450 cm during rainy season from October 1 to April 30
Frequency	Interannual flood occurrence	Number of previous years without flood (level ≥ 450 cm)

Flow Regime Index Model

This subroutine calculates flow regime indexes (metrics) from the flow regime options generated in Subroutine 1. The model represents each component of a flow regime (duration, magnitude, timing, frequency, and rate of change) by indexes that must be chosen according to the ecological function modeled. For the study area, nine indexes were selected, at least one index for each component (Table 1), to represent the dry and rainy seasons and conditions historically linked to fish migration and initial growth of migratory species.

Previous studies of Suzuki et al. (2009) and Oliveira et al. (2015, 2020) supported the specification of the indexes' thresholds. The indexes representing the flood season duration (FSD) were divided into three main magnitude ranges in order to represent different floodplain connections during the flood season: (1) the index *FSD low magnitude* considers the level between 450 and 540 cm the minimum range to allow lateral and longitudinal connectivity in the floodplain during the rainy season, (2) the index *FSD midmagnitude* considers the level between 540 and 610 cm as the intermediary connectivity, and (3) the index *FSD high magnitude* treats the 610 cm level as the threshold level that allows high connectivity along the floodplain.

The dry season duration is represented by the index DSD, which treats the level of 250 cm as the water threshold level governed by the baseflow (historical Q_{80} flow duration). The flow regime timing component is represented by the *flood delay* index, and the rate of change (variability) is represented by the *uninterrupted flood duration* and the *number of flood pulses* indexes. The uninterrupted flood duration index indicates how the flood pulses are spatially distributed in time (e.g., long uninterrupted flood duration is produced by time distant pulses). The *interannual flood occurrence* index represents the frequency component. The relevance of each index is analyzed in Appendix IV.

Fish Abundance Model

ANNs are data-driven computational networks able to establish empirical relationships between independent (input) and dependent (output) variables (Sadiq et al. 2019) with the advantage of not being limited by a prespecified functional form (Adamowski and Karapataki 2010). The ANN model developed to predict the YoY fish abundance from different flow regime options consists of three layers: an input layer, a hidden layer, and an output layer (Fig. 5).

The input layer has nine nodes representing the set of annual flow regime indexes calculated by the flow regime indexes model (Subroutine 2). The input layer distributes the input signals via connections to each hidden neuron. Each connection has a weight, w, adjusted via training, and each neuron has an activation function, f. Neurons process the sum of impinging signals from previous layers and independent terms, b, with the activation function, and each output neuron sends its output signal to the respective output node. The output note is represented by the annual YoY fish abundance of the floodplain.

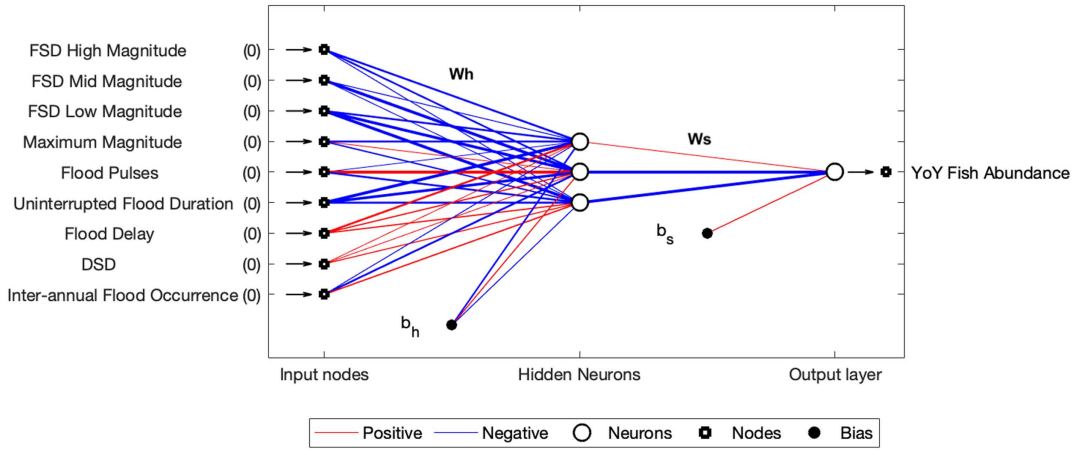

Fig. 5. Representation of ANN model architecture.

Table 2. ANN parameters

Parameter	Description
Architecture	9 - hn - 1
Input variables	Flow regime indexes
Output variable	YoY fish abundance
Number of hidden neurons (hn)	3 (chosen according to complexity analysis)
Activation function	Sigmoid unipolar, $f(x) = 1/(1 + e^{-x})$
Input data scaling	Linear (amplitude), [0,1]
Data time step	Annual

The input and output data are linearly scaled to fit the domain range [0,1] whose scaling parameters are the respective global maximum and minimum of each variable in the data set. Table 2 summarizes the main parameters used to configure the ANN model. We investigated the number of hidden neurons (*hn*) necessary to present a performance similar to an oversized ANN by testing different numbers of hidden neurons and evaluating the final overall performance.

To predict the YoY fish abundance from different flow regime options, the ANN model required to be first trained and validated based on the historical data. The registers (individual input–output pairs) from 1991 to 1993 and from 1999 to 2018 composed the data set (the year number corresponds to the year the flood season begins; see Appendix II).

To prevent overfitting and to overcome the challenge of working with a small data set, we applied a nested leave-one-out cross-validation (NLCV) training approach (Wong 2015). This approach (Appendix III) consisted in using the data set with different configurations of registers divided a between training set (TS) and verification set (VS) and training each configuration separately to check the consistency of the model to produce similar results between configurations, which corroborates its generalizability to new data. The final data set was arranged in 3 configurations, each with 6 registers for the verification set and 17 registers for the training set (Fig. 6). Years with unique features (Appendix II) were included in the training set to improve the model's ability to recognize such behavior.

The trained ANN model integrated the model's Subroutine 3 with the objective of calculating the corresponding YoY fish abundance of each flow regime option designed in Subroutine 1. To reduce the number of combinations assessed in this study, we discarded flow regime options with very close characteristics in terms of fish abundance and reservoir operation decisions. The final options were termed functional flow regimes, arranged in hydrographs.

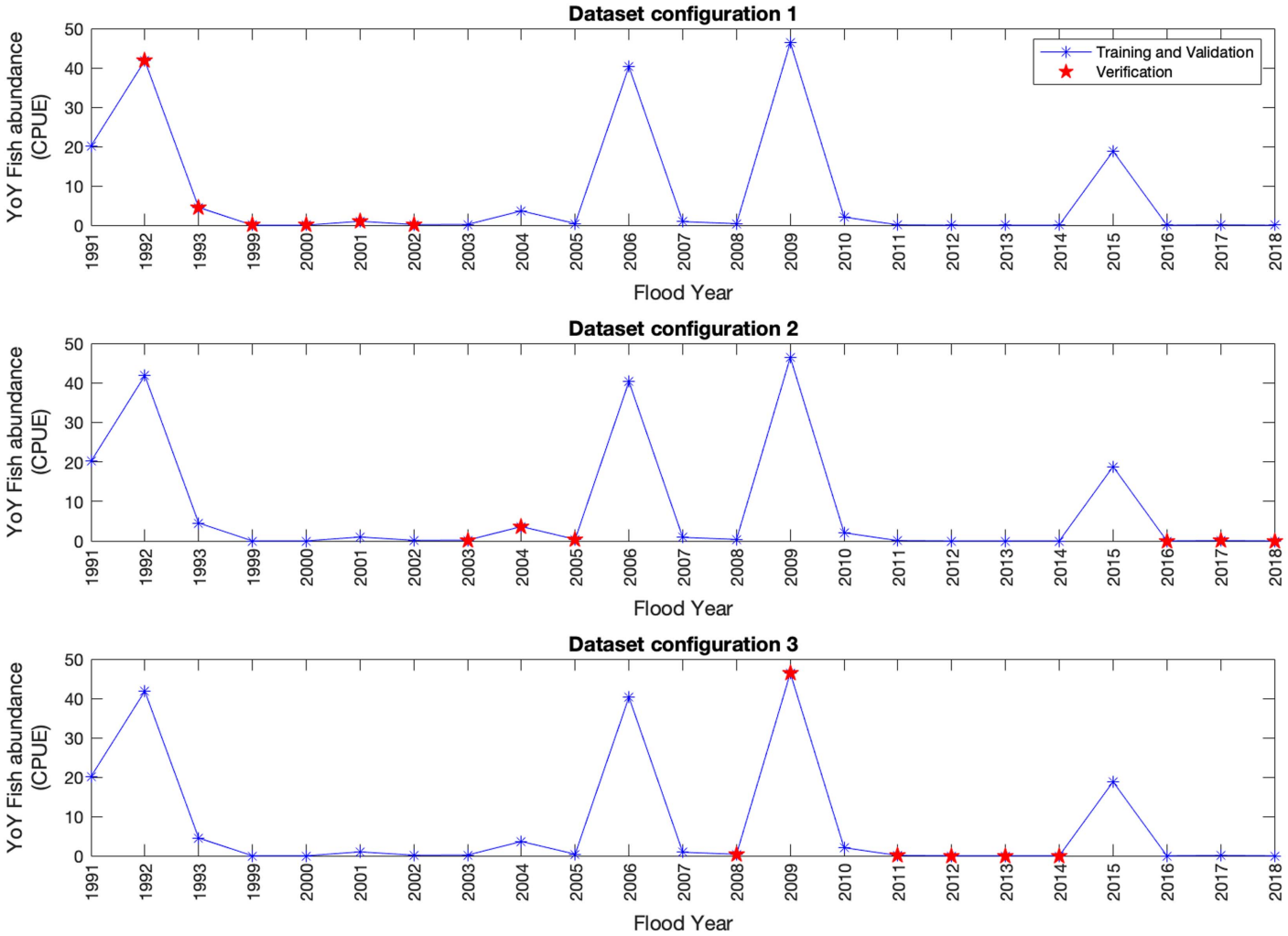

Fig. 6. Training and verification registers for each data set configuration.

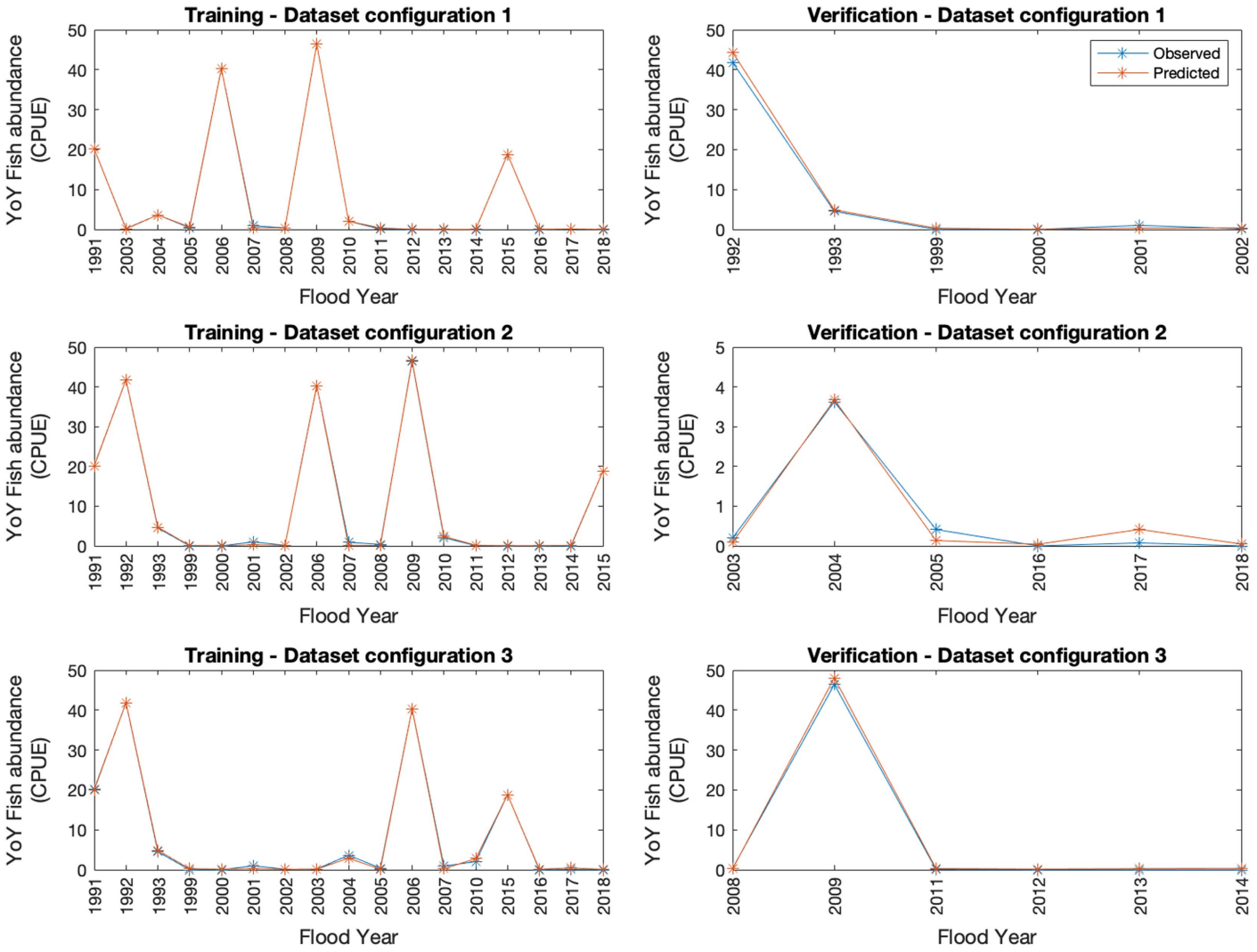

Fig. 7. Annual comparison of predicted and observed fish abundance for each data set configuration.

Results and Discussion

Performance Analysis of Fish Abundance Model

Figs. 7 and 8 present a comparison of the observed and predicted results for the training and verification sets of the three data set configurations. Four years of the data set present unique features, which required them to be included in the training set during the ANN model training and validation to improve the model's ability to recognize such behavior. Although the model was able to train, there are no data with similar features in the verification set to check the prediction performance. This aspect may have influenced the metrics' good results, while the model's capability to generalize to new data depends on more future information and monitoring data.

However, the ANN model was able to satisfactorily reproduce the peak abundance behavior of the verification sets, although most training registers correspond to YoY fish abundances below 4 CPUE, which indicates the model's robustness in defining clear objectives for ecosystem management by focusing on key flow regime components.

The negative verification mean error (ME) of the performance analysis indicates that the model overall underestimates the fish abundance (Table 3). The maximum absolute verification error (Emax = 0.688 CPUE) indicates that the model presents good performance in predicting high fish abundance values. This error represents less than 2% of the fish abundance peak of this data set configuration (41.8 CPUE). The NS and R^2 performance coefficients also indicate the model can reproduce low and high fish abundance variations with good performance.

Functional Flow Regimes Analysis

We chose six functional flow regimes for analysis (Fig. 9), which allowed us to identify distinct fish abundance performances (graphs' rightside bar) comparing the different functional flow regimes (graphs' continuous line) and analyze the implications from the perspective of reservoirs' release decisions. The corresponding flow regime indexes of each functional flow regime are detailed in Table 4.

FH1 represents a scenario in which upstream reservoirs' release decisions are made to get close to the natural flow regime upper bound (favoring high flood magnitudes and duration and low flood variability and delay). The longer the period of high water levels, the greater the possibility that juveniles will remain in the floodplain for feeding and be less susceptible to predation, improving conditions for recruitment success. The result is a high YoY fish abundance response.

However, in terms of hydropower operation, high reservoir outflow releases in the rainy season to sustain fish recruitment

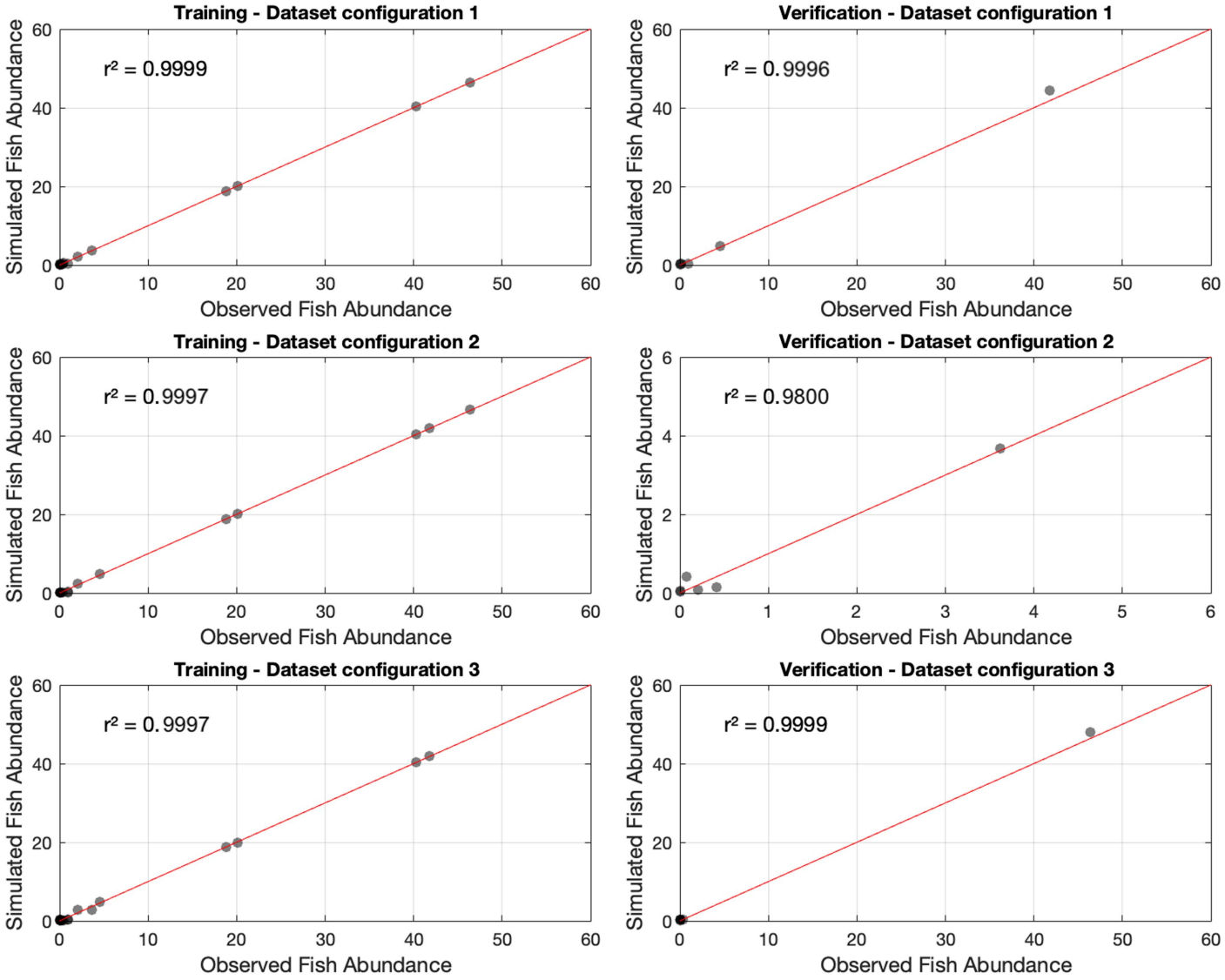

Fig. 8. Comparison of predicted and fish abundance for each data set configuration.

Table 3. Model performance analysis

Data set configuration	Set	Nash–Sutcliffe coefficient (NS)	ME (ME)	Root mean square error (RMSE)	Coefficient of determination (R^2)	Maximum error (E_{max})
1	Training	0.9999	0.0023	0.4328	0.9999	0.487
	Verification	0.9948	−1.3781	3.2898	0.9996	0.688
2	Training	0.9997	0.1281	0.8618	0.9997	0.773
	Verification	0.9794	−0.0465	0.5626	0.9800	0.277
3	Training	0.9997	0.0123	0.6837	0.9997	0.602
	Verification	0.9965	−1.4490	3.0455	0.9999	0.130

may delay reservoir refilling, increasing the risk of future storage deficit and hydropower production. Converting level into streamflow by the rating curve and comparing the other functional flows (FH2 to FH6) to FH1 make it possible to estimate the change in annual storage upstream and how the energy trade-off can be mitigated by changing the characteristics of the flow released, while still producing YoY fish abundance. The lower the water levels of a given FH compared to FH1, the lower the flow release and the more storage can be maintained upstream to either meet demand for other water uses or improve drought protection in the next year.

In FH5, the reservoir release is reduced mostly in January and February to produce lower flood level magnitudes compared to FH1 while maintaining flood duration, variability, and delay. This shows that high performance (YoY fish abundance) can still be achieved without outflow releases as significant as FH1. Once a minimum flood threshold level is reached, the floodplain connections already provide sufficient access to food and shelter for juvenile fish development, which leads to good results in fish abundance. From this magnitude on, there are diminishing returns to further change reservoir operation and recover the magnitude of the flow regime, considering fish abundance.

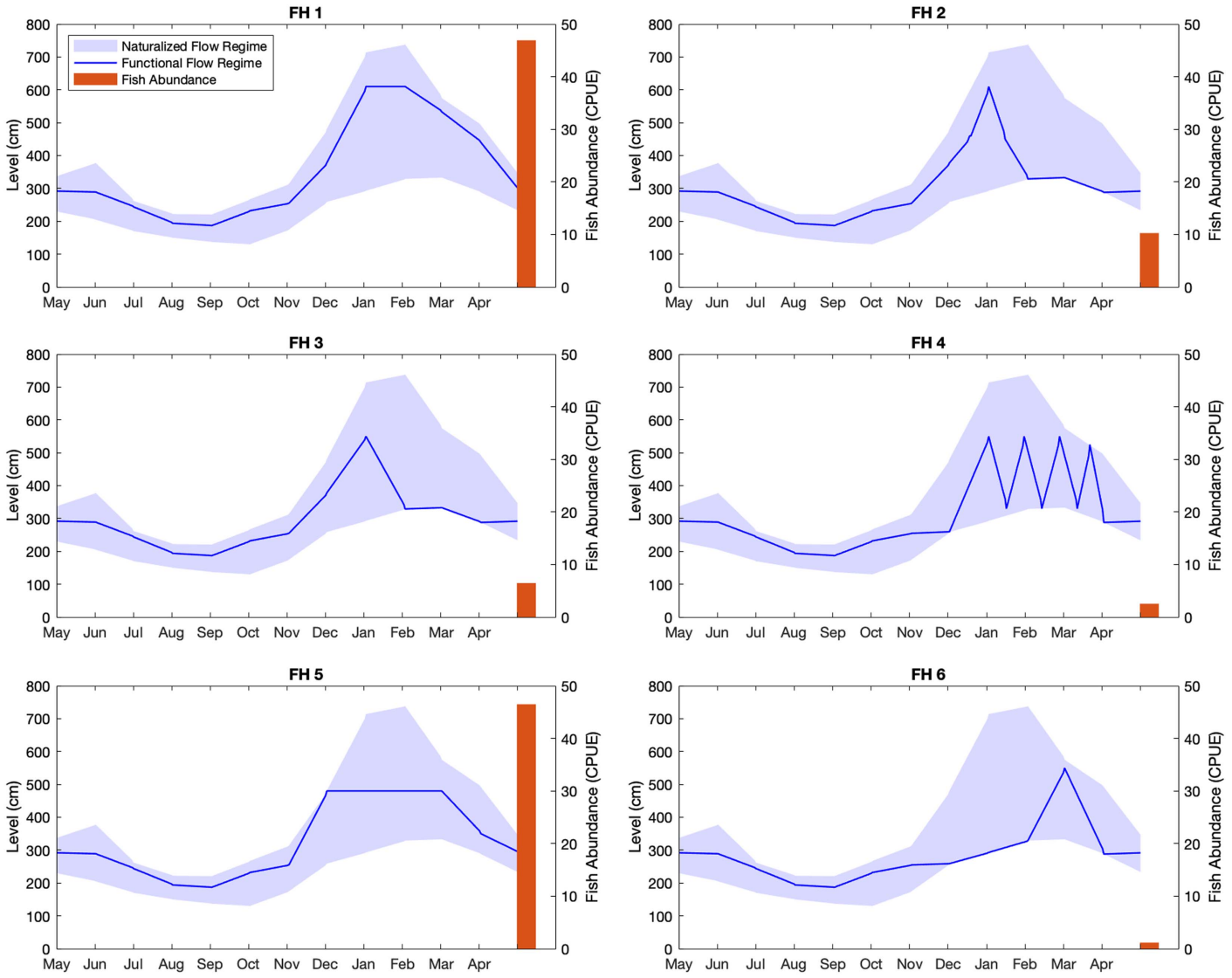

Fig. 9. Functional flow regimes and corresponding YoY fish abundance.

Table 4. Flow regime indexes of each functional flow regime

FH	FSD high magnitude (days)	FSD midmagnitude (days)	FSD low magnitude (days)	Maximum magnitude (cm)	Flood pulses (cycles)	Uninterrupted flood duration (days)	Flood delay (days)	DSD (days)	Interannual flood occurrence (years)	YoY fish abundance (CPUE)
1	32	35	43	610	1	110	71	96	0	46.7
2	1	12	17	610	1	30	76	96	0	10.3
3	0	2	30	550	1	32	75	96	0	6.5
4	0	3	45	550	4	18	81	96	0	2.6
5	0	0	100	480	1	100	58	96	0	46.0
6	0	2	23	550	1	25	140	96	0	1.2

For upstream reservoir operation, this result is very important because it means significant ecosystem recovery can still be achieved without necessarily using as much storage from upstream reservoirs as in FH1. The annual surplus of 24,782 hm^3 can be kept in upstream storage to maintain power generation later in the year and also help meeting other demands. Part of the Upper Paraná River Basin of approximately 460,000 ha of irrigated crops could benefit from higher storage, especially during drought years.

In FH2, releases are still capable of reaching a high flood level magnitude that is similar to that of FH1, but with shorter durations, maintaining similar flood delay and variability. With less time to develop and access shelter and food in the floodplain, juveniles return to the main channels more susceptible to predators, affecting recruitment. The YoY fish abundance response is then reduced by 78%, a significant performance loss. Despite this, the resulting fish abundance is above 10 CPUE, which is still relevant, considering that in 23 years of sampling collection just 5 years had YoY fish

abundances above 10 CPUE. The 62,533 hm^3 in increased annual water storage upstream may be useful in drought years, when system storage is severely limited and the risk of near future energy and water deficits is high.

In FH3, the releases produce a flood magnitude slightly lower than FH2, but with a similar total duration above the FSD low magnitude. Although YoY fish abundance is further reduced from FH2, it may be another intermediate option, adequate for scenarios whose reservoir storage must be guaranteed to reduce future hydropower deficit risk (increase of 52,064 hm^3 in upstream storage) but still producing relevant YoY fish abundance (above 6 CPUE).

FH4 represents a scenario whose flood magnitude is similar to that of FH3 but with higher variability and delay than FH3. Release decisions that produce such behavior in the floodplain should be avoided since the YoY fish abundance response is very low and the trade-offs for reservoir operation may be less beneficial than other scenarios. High water level variabilities increase the risk of predation and induce resorption of gonads, affecting spawning. The 44,384 hm^3 in increased annual water storage upstream is close to the FH3 result; however, the YoY fish abundance response is reduced, which indicates that similar water storage can be obtained by managing timing and variability and with better YoY fish abundance response than the one shown in FH4.

Finally, in FH6 release decisions produce a moderate flood duration with a long delay. Delaying the flood by more than 140 days causes it to miss a critical time window for gonadal maturation and upstream migration. A flood that comes too late resulted in the worst performance in fish abundance and should also be avoided. Instead, anticipating the same flow release in 1 or 2 months would produce better YoY fish response, as shown in FH2 and FH3.

Conclusion

The proposed methodology framework investigated how functional flow regimes can be generated, organized according to specific flow components, and measure their performance in terms of fish response. Some specific conclusions are possible, as follows:

1. Different combinations of flow regime components bring different ecological response performances. While flow magnitude and duration are key contributors to performance for the ecological function modeled, there is a clear threshold above which performance gains are smaller.
2. The preceding conclusion indicates the presence of diminishing marginal performance gains in the design of an environmental flow, which is important when the trade-offs between options are incorporated into flow allocation discussions on competing uses.
3. Although not always reaching the best response level, relevant YoY fish abundance can still be achieved when combining different flow regime components. This indicates that there is some flexibility in system operation. This flexibility should be explored, with the help of the results provided by the methods proposed here, in the preparation of more robust ecosystem restoration plans.
4. Some options should clearly be avoided because their performance in terms of fish abundance is very low.

All these conclusions highlight the notion that restoring flow regimes to improve ecosystem services is a water allocation exercise. Once several functional flows are designed, users will know how much water—and when and under which variation pattern—is necessary to attain different levels of performance. This is the starting point to support water managers in exploring alternative reservoir operating schemes that perform well in releasing water in connection with YoY fish abundance relative to other system objectives. The proposed framework is flexible, which allows its application to other areas and ecological functions by changing the input hydrological time series and adjusting the flow regime indexes.

Appendix I. Naturalized Flow Regime Estimation

A three-step procedure was adopted to generate the naturalized flow regime in the study area. First, the altered time series of daily flow upstream (Porto Primavera and Rosana power plants) were correlated with the respective altered time series of daily level downstream (at Porto São Jose gauging station) with a multiple linear regression [Eq. (1)]. The resulting coefficient of determination (R^2) of 0.923 indicated that both independent variables could satisfactorily explain the level at Porto São José station

$$L_{PSJ} = 0.03709 \cdot Q_{PM} + 0.03217 \cdot Q_{ROS} - 6.9733 \quad (1)$$

where L_{PSJ} = level at Porto São José station (cm); Q_{PM} = flow at Porto Primavera (m^3/s); and Q_{ROS} = flow at Rosana (m^3/s).

Second, Eq. (1) was used to estimate the naturalized time series of daily level downstream (at Porto São Jose gauging station), using as input the naturalized flow time series upstream (Porto Primavera and Rosana power plants) obtained from the Brazilian Independent System Operator (ONS) (ANA 2020b), which reverts the flow regulation effects and evaporation losses of the reservoirs part of the hydropower system. Because Eq. (1) includes levels at a maintained stage-discharge station, it is transferable across different naturalized flow input data. Finally, the estimated naturalized time series of daily level downstream (at Porto São Jose station) was used to identify the range of the regime variability in an annual period (outliers were removed).

Appendix II. Flow Regime Index Analysis

Table 5 presents the resulting flow regime indexes for each year of the observed level time series at the Porto São José station with the corresponding observed floodplain YoY fish abundance.

Four years with unique features were observed in the data set (2006, 2015, 2010, 1991). The year 2006 presented the long duration for magnitude levels above 610 cm (FSD high magnitude) and short duration for low and intermediate flood magnitudes (FSD low magnitude and FSD midmagnitude). The other years showed the opposite behavior (higher low and intermediate magnitude durations).

The year 2015 showed high YoY fish abundance (above 15 CPUE), although not presenting significant flood durations in the three magnitude ranges (total of 26 days above the 450 cm level). Two main aspects may have contributed to this particular result: (1) the number of previous years without flood (highest record); and (2) the flood duration in the Ivinhema tributary. The flood duration in the Ivinhema was 190 days during the 2015 flood season (the highest data set record), in which 26 days were combined with a flood in the Paraná River. Because it is difficult to distinguish the YoY fish abundance related just to the specific subsystem (fish tend to disperse through floodplain), the result may have suffered a predominant influence of the great Ivinhema flood in that year.

On the other hand, the year 2010, although presenting considerable flood duration (43 days above the 450 cm level), resulted in low YoY fish abundance (2.05 CPUE). The previous year's great

Table 5. Flow regime indexes calculated for the Paraná River target reach

Flood year[a]	FSD high magnitude (days)	FSD midmagnitude (days)	FSD low magnitude (days)	Maximum magnitude (cm)	Flood pulses (cycles)	Uninterrupted flood duration (days)	Flood delay (days)	DSD (days)	Interannual flood occurrence (years)	YoY fish abundance (CPUE)
1985	0	0	0	365	0	0	365	0	0	N/A
1986	0	0	0	430	0	0	365	19	1	N/A
1987	0	7	37	584	6	15	103	11	2	N/A
1988	0	10	32	602	3	23	105	4	0	N/A
1989	24	6	10	790	2	35	84	0	0	N/A
1990	19	23	16	696	2	37	125	24	0	N/A
1991	3	16	31	613	4	29	117	0	0	20.15
1992	16	6	71	664	6	44	42	0	0	41.82
1993	0	9	20	606	2	24	109	2	0	4.52
1994	14	8	13	652	2	26	104	1	0	N/A
1995	0	0	2	476	1	2	161	6	0	N/A
1996	28	10	8	853	1	46	103	12	0	N/A
1997	2	9	41	618	4	22	151	0	0	N/A
1998	0	7	39	598	12	13	0	0	0	N/A
1999	0	0	4	508	1	4	175	3	0	0.00
2000	0	0	0	414	0	0	365	11	0	0.00
2001	0	0	12	530	3	9	138	92	1	1.00
2002	0	0	11	502	3	7	121	82	0	0.15
2003	0	0	3	481	1	3	199	48	0	0.20
2004	14	6	13	726	2	30	105	42	0	3.62
2005	0	0	20	512	7	8	81	37	0	0.41
2006	46	5	6	679	1	57	103	5	0	40.31
2007	0	0	10	497	2	9	178	20	0	0.91
2008	0	0	5	506	2	4	149	2	0	0.38
2009	40	32	31	741	5	75	16	28	0	46.42
2010	18	8	17	726	5	29	113	10	0	2.05
2011	0	0	4	487	1	4	120	6	0	0.08
2012	0	0	0	428	0	0	365	2	0	0.00
2013	0	0	0	402	0	0	365	23	1	0.00
2014	0	0	0	328	0	0	365	93	2	0.00
2015	2	6	18	637	3	12	91	92	3	18.80
2016	0	0	0	402	0	0	365	31	0	0.00
2017	0	0	4	473	1	4	110	76	1	0.08
2018	0	0	0	348	0	0	365	93	0	0.00

[a]The year corresponds to the year the flood season begins.

flood (highest data set register) may have influenced this result (the opposite case of 2015) through factors and conditions not studied here. Finally, the year 1991 presented a high fish abundance, although with a high flood delay.

Appendix III. Artificial Neural Network Training Procedure

Fig. 10 depicts the NLCV procedure used for training and verifying the performance of the fish abundance model. The data set configurations between the TS and VS composed an outer loop, and for each iteration n, the $VS_{(n)}$ set was saved, while $TS_{(n)}$ was trained in an inner loop by applying the leave-one-out (LOO) technique, which consisted in leaving one nonzero register, j, out for checking the error (validation set) and using the remaining ones for the training process. For each iteration j of the inner loop, training was ceased, and the weights recorded when the validation error stopped improving to prevent overfitting. Finally, the weights and biases (w and b) that resulted in the best performance among the inner loop iterations were applied to the corresponding verification set $VS_{(n)}$ in order to evaluate the performance of each configuration of the outer loop.

The ANN training procedure was based on feedforward backpropagating the error (Rumelhart et al. 1986) and subsequently adjusting the weights based on the delta rule (Widrow and Hoff 1960). The momentum factor and dynamic learning rate were applied as accelerating methods (Vogl et al. 1988). To minimize the ANNs' limitation in extrapolating the domain of the training set, registers with unique features were assigned to the training set (see Appendix II for more details).

Appendix IV. Flow Regime Index Relevance

We checked the performance response of the model to each flow regime index as an indication of its contribution to explain the observed fish abundance (Lek et al. 1996). The ANN model data set was retrained leaving one input variable out at each simulation (Table 6).

The *FSD low magnitude*, *FSD midmagnitude*, and *flood pulses* indexes had a significant effect on performance, indicating that flood duration and variability play an important role in migratory fish recruitment. The *interannual flood occurrence* index must be analyzed with caution. Just one data set register, from 2016, is characterized as having three previous years without flood, which may not be generalized for other events. The high abundance of this year might have been affected by other conditions not analyzed here that triggered high rates of fish reproduction despite not having the best flooding index conditions. The low performance reduction of the

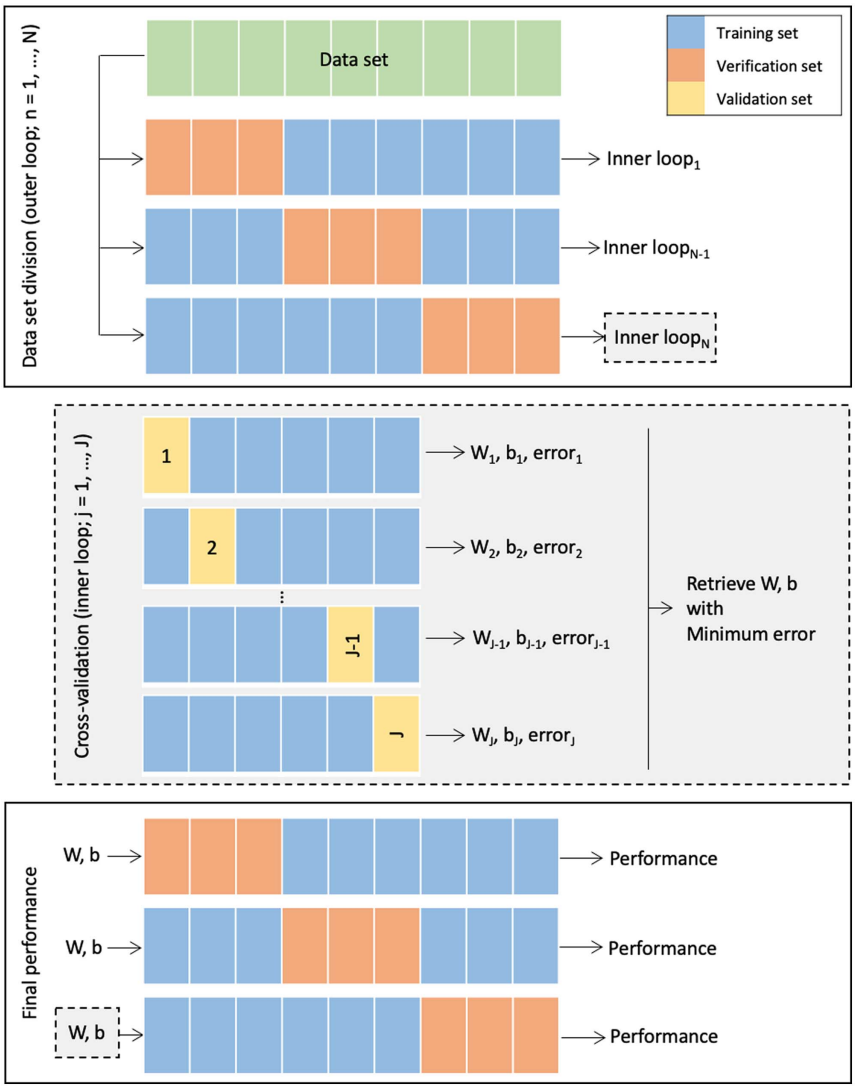

Fig. 10. Nested leave-one-out cross-validation procedure.

Table 6. Average performance reduction analysis for each input variable removed

Input variable removed	R^2	Performance reduction (%)	Nash–Sutcliffe coefficient (NS)	Performance reduction (%)
None	0.993	—	0.990	—
FSD high magnitude	0.992	−0.1	0.941	−5.0
FSD midmagnitude	0.843	−15.2	0.754	−23.9
FSD low magnitude	0.913	−8.1	0.540	−45.5
Maximum magnitude	0.992	−0.1	0.941	−5.0
Flood pulses	0.712	−28.3	0.690	−30.3
Uninterrupted flood duration	0.992	−0.1	0.980	−1.0
Flood delay	0.993	−0.1	0.906	−8.5
DSD	0.993	0.0	0.944	−4.6
Interannual flood occurrence	0.990	−0.3	−5.096	−614.7

DSD index may indicate that low water level season affects fish recruitment indirectly. One way for this to happen is by allowing more vegetation growth during the dry season, which would result in increased food and shelter in the next flood season (Agostinho et al. 2000). However, the results do not allow a clear relationship to be defined.

Data Availability Statement

Some or all data, models, or code that support the findings of this study are available from the corresponding author upon reasonable request. Items available: fish sampling data and framework routine codes. Flow/level data are publicly available on the reference websites.

Acknowledgments

The authors thank the Inter-American Institute for Global Change Research (IAI) for financial support under SGP-HW program, project SGP-HW 091, and CNPq for financial support through Grant 552 308549/2019-8. The authors are also grateful to Professor Olavo C. Pedrollo and engineer Juliano S. Finck for discussions on the ANN approach.

References

Adamowski, J., and C. Karapataki. 2010. "Comparison of multivariate regression and artificial neural networks for peak urban water-demand forecasting: Evaluation of different ANN learning algorithms." *J. Hydrol. Eng.* 15 (10): 729–743. https://doi.org/10.1061/(ASCE)HE.1943-5584.0000245.

Adams, L. E., J. R. Lund, P. B. Moyle, R. M. Quiñones, J. D. Herman, and T. A. O'Rear. 2017. "Environmental hedging: A theory and method for reconciling reservoir operations for downstream ecology and water supply." *Water Resour. Res.* 53 (9): 7816–7831. https://doi.org/10.1002/2016WR020128.

Agostinho, A. A., F. M. Pelicice, A. C. Petry, L. C. Gomes, and H. F. Júlio. 2007. "Fish diversity in the upper Paraná River basin: Habitats, fisheries, management and conservation." *Aquat. Ecosyst. Health Manage.* 10 (2): 174–186. https://doi.org/10.1080/14634980701341719.

Agostinho, A. A., S. M. Thomaz, C. V. Minte-Vera, and K. O. Winemiller. 2000. "Biodiversity in the high Paraná River floodplain." In *Biodiversity in wetlands: Assessment, function and conservation*. London: Backhuys Publishers.

ANA (Agência Nacional de Águas). 2020a. "Hidroweb." Accessed February 1, 2020. http://www.snirh.gov.br/hidroweb/apresentacao.

ANA (Agência Nacional de Águas). 2020b. "SAR—Sistema de acompanhamento de reservatórios." Accessed February 15, 2020. https://www.ana.gov.br/sar/.

Arthington, A. H., A. Bhaduri, S. E. Bunn, S. E. Jackson, R. E. Tharme, and D. Tickner. 2018. "The Brisbane declaration and global action agenda on environmental flows (2018)." *Front. Environ. Sci.* 6 (Jul): 45. https://doi.org/10.3389/fenvs.2018.00045.

Arthington, A. H., S. E. Bunn, N. L. Poff, and R. J. Naiman. 2006. "The challenge of providing environmental flow rules to sustain river ecosystems." *Ecol. Appl.* 16 (4): 1311. https://doi.org/10.1890/1051-0761(2006)016[1311:TCOPEF]2.0.CO;2.

CCEE (Câmara de Comercialização de Energia Elétrica). 2020. "Hydroedit—Apoio à leitura de arquivos." Accessed December 10, 2020. https://www.ccee.org.br/portal/faces/pages_publico/o-que-fazemos/como_ccee_atua/precos/deck_de_precos.

Chen, W., and J. D. Olden. 2017. "Designing flows to resolve human and environmental water needs in a dam-regulated river." *Nat. Commun.* 8 (1): 2158. https://doi.org/10.1038/s41467-017-02226-4.

Comunello, É., P. C. Rocha, and M. R. Nanni. 2003. "Dinâmica de inundação de áreas sazonalmente alagáveis na planície aluvial do Alto Rio Paraná: Estudo preliminar." In *Simpósio Brasileiro De Sensoriamento Remoto*. Belo Horizonte, Brasil: INPE.

Cooper, A. R., D. M. Infante, W. M. Daniel, K. E. Wehrly, L. Wang, and T. O. Brenden. 2017. "Assessment of dam effects on streams and fish assemblages of the conterminous USA." *Sci. Total Environ.* 586 (2): 879–889. https://doi.org/10.1016/j.scitotenv.2017.02.067.

Crespo, D., J. Albiac, T. Kahil, E. Esteban, and S. Baccour. 2019. "Trade-offs between water uses and environmental flows: A hydroeconomic analysis in the Ebro Basin." *Water Resour. Manage.* 33 (7): 2301–2317. https://doi.org/10.1007/s11269-019-02254-3.

Fernandes, J. A., X. Irigoien, N. Goikoetxea, J. A. Lozano, I. Inza, A. Pérez, and A. Bode. 2010. "Fish recruitment prediction, using robust supervised classification methods." *Ecol. Modell.* 221 (2): 338–352. https://doi.org/10.1016/j.ecolmodel.2009.09.020.

Freeman, M. C., Z. H. Bowen, K. D. Bovee, and E. R. Irwin. 2001. "Flow and habitat effects on juvenile fish abundance in natural and altered flow regimes." *Ecol. Appl.* 11 (2): 631. https://doi.org/10.1890/1051-0761(2001)011[0179:FAHEOJ]2.0.CO;2.

Grantham, T. E., J. Mount, E. D. Stein, and S. Yarnell. 2020. *Making the most of water for the environment: A functional flows approach for California's Rivers*. San Francisco: Public Policy Institute of California.

Grill, G., B. Lehner, A. E. Lumsdon, G. K. MacDonald, C. Zarfl, and C. Reidy Liermann. 2015. "An index-based framework for assessing patterns and trends in river fragmentation and flow regulation by global dams at multiple scales." *Environ. Res. Lett.* 10 (1): 015001. https://doi.org/10.1088/1748-9326/10/1/015001.

Harwood, A., S. Johnson, B. Richter, A. Locke, X. Yu, and D. Tickner. 2017. *Listen to the river: Lessons from a global review of environmental flow success stories*. Woking, UK: World Wildlife Fund-UK.

Holmlund, C. M., and M. Hammer. 1999. "Ecosystem services generated by fish populations." *Ecol. Econ.* 29 (2): 253–268. https://doi.org/10.1016/S0921-8009(99)00015-4.

Howard, J. K., K. A. Fesenmyer, T. E. Grantham, J. H. Viers, P. R. Ode, and P. B. Moyle. 2018. "A freshwater conservation blueprint for California: Prioritizing watersheds for freshwater biodiversity." *Freshwater Sci.* 37 (2): 417–431. https://doi.org/10.1086/697996.

Hu, J. H., W. P. Tsai, S. T. Cheng, and F. J. Chang. 2020. "Explore the relationship between fish community and environmental factors by machine learning techniques." *Environ. Res.* 184 (1): 109262. https://doi.org/10.1016/j.envres.2020.109262.

Joy, M. K., and R. G. Death. 2004. "Predictive modelling and spatial mapping of freshwater fish and decapod assemblages using GIS and neural networks." *Freshwater Biol.* 49 (8): 1036–1052. https://doi.org/10.1111/j.1365-2427.2004.01248.x.

Lek, S., A. Belaud, P. Baran, I. Dimopoulos, and M. Delacoste. 1996. "Role of some environmental variables in trout abundance models using neural networks." *Aquat. Living Resour.* 9 (1): 23–29. https://doi.org/10.1051/alr:1996004.

Li, F.-F., J.-H. Wei, J. Qiu, and H. Jiang. 2020. "Determining the most effective flow rising process to stimulate fish spawning via reservoir operation." *J. Hydrol.* 582 (Mar): 124490. https://doi.org/10.1016/j.jhydrol.2019.124490.

Loures, R. C., and P. S. Pompeu. 2018. "Long-term study of reservoir cascade in south-eastern Brazil reveals spatio-temporal gradient in fish assemblages." *Mar. Freshwater Res.* 69 (12): 1983. https://doi.org/10.1071/MF18109.

Marques, G. F., and A. Tilmant. 2018. "Cost distribution of environmental flow demands in a large-scale multireservoir system." *J. Water Resour. Plann. Manage.* 144 (6): 04018024. https://doi.org/10.1061/(ASCE)WR.1943-5452.0000936.

McKay, S. K., I. Linkov, J. C. Fischeinch, S. J. Miller, and L. J. Valverde. 2012. *Ecosystem restoration objectives and metrics*. Athens, GA: US Army Engineer Research and Development Center.

Moyle, P. B., J. V. E. Katz, and R. M. Quiñones. 2011. "Rapid decline of California's native inland fishes: A status assessment." *Biol. Conserv.* 144 (10): 2414–2423. https://doi.org/10.1016/j.biocon.2011.06.002.

Olden, J. D., and N. L. Poff. 2003. "Redundancy and the choice of hydrologic indices for characterizing streamflow regimes." *River Res. Appl.* 19 (2): 101–121. https://doi.org/10.1002/rra.700.

Oliveira, A. G., H. I. Suzuki, L. C. Gomes, and A. A. Agostinho. 2015. "Interspecific variation in migratory fish recruitment in the Upper Paraná River: Effects of the duration and timing of floods." *Environ. Biol. Fishes* 98 (5): 1327–1337. https://doi.org/10.1007/s10641-014-0361-5.

Oliveira, A. G. D., T. M. Lopes, M. A. Angulo-Valencia, R. M. Dias, H. I. Suzuki, I. C. B. Costa, and A. A. Agostinho. 2020. "Relationship of freshwater fish recruitment with distinct reproductive strategies and flood attributes: A long-term view in the Upper Paraná River floodplain." *Front. Environ. Sci.* 192 (Sep): 98. https://doi.org/10.3389/fenvs.2020.577181.

Ota, R. R., G. Deprá, C. de, W. J. Graça, and C. S. Pavanelli. 2018. "Peixes da planície de inundação do alto rio Paraná e áreas adjacentes: Revised, annotated and updated." *Neotrop. Ichthyol.* 16 (2): 11. https://doi.org/10.1590/1982-0224-20170094.

Palmer, M., and A. Ruhi. 2019. "Linkages between flow regime, biota, and ecosystem processes: Implications for river restoration." *Science* 365 (6459): eaaw2087. https://doi.org/10.1126/science.aaw2087.

Piffady, J., Y. Souchon, H. Capra, and E. Parent. 2010. "Quantifying the effects of temperature and flow regime on the abundance of 0+ cyprinids

in the upper River Rhone using Bayesian hierarchical modelling." *Freshwater Biol.* 55 (11): 2359–2374. https://doi.org/10.1111/j.1365-2427.2010.02453.x.

Poff, N. L., J. D. Allan, M. B. Bain, J. R. Karr, K. L. Prestegaard, and B. D. Richter. 1997. "The natural flow regime." *Bioscience* 47 (11): 769–784. https://doi.org/10.2307/1313099.

Poff, N. L., R. E. Tharme, and A. H. Arthington. 2017. "Evolution of environmental flows assessment science, principles, and methodologies." *Water Environ.* 12 (6): 203–236. https://doi.org/10.1016/B978-0-12-803907-6.00011-5.

Pringle, C. M., M. C. Freeman, and B. J. Freeman. 2000. "Regional effects of hydrologic alterations on riverine Macrobiota in the new world: Tropical–temperate comparisons." *BioScience* 50 (9): 807–823. https://doi.org/https://doi.org/10.1641/0006-3568(2000)050[0807:REOHAO]2.0.CO;2.

Quesne, L., E. Kendy, and D. Weston. 2010. "The implementation challenge—Taking stock of government policies to protect and restore environmental flows." Accessed July 10, 2021. http://www.conservationgateway.org/Documents/GlobalflowsreportfinalLowRes.pdf.

Rumelhart, D. E., G. E. Hinton, and R. J. Williams. 1986. "Learning representations by back-propagating errors." *Nature* 323 (6088): 533–536. https://doi.org/10.1038/323533a0.

Sadiq, R., M. J. Rodriguez, and H. R. Mian. 2019. "Empirical models to predict disinfection by-products (DBPs) in drinking water: An updated review." In *Encyclopedia of environmental health*, 324–338. Amsterdam, Netherlands: Elsevier.

Suen, J.-P., and J. W. Eheart. 2006. "Reservoir management to balance ecosystem and human needs: Incorporating the paradigm of the ecological flow regime." *Water Resour. Res.* 42 (Mar): 312–318. https://doi.org/10.1029/2005WR004314.

Suzuki, H., A. Agostinho, D. Bailly, M. Gimenes, H. Júlio-Junior, and L. Gomes. 2009. "Inter-annual variations in the abundance of young-of-the-year of migratory fishes in the Upper Paraná River floodplain: Relations with hydrographic attributes." *Braz. J. Biol.* 69 (2): 649–660. https://doi.org/10.1590/S1519-69842009000300019.

Tharme, R. E. 2003. "A global perspective on environmental flow assessment: Emerging trends in the development and application of environmental flow methodologies for rivers." *River Res. Appl.* 19 (5–6): 397–441. https://doi.org/10.1002/rra.736.

Tilmant, A., D. Arjoon, and G. F. Marques. 2014. "Economic value of storage in multireservoir systems." *J. Water Resour. Plann. Manage.* 140 (3): 375–383. https://doi.org/10.1061/(ASCE)WR.1943-5452.0000335.

Tonkin, Z., J. Yen, J. Lyon, A. Kitchingman, J. D. Koehn, and W. M. Koster. 2021. "Linking flow attributes to recruitment to inform water management for an Australian freshwater fish with an equilibrium life-history strategy." *Sci. Total Environ.* 752 (Mar): 141863. https://doi.org/10.1016/j.scitotenv.2020.141863.

Vogl, T. P., J. K. Mangis, A. K. Rigler, W. T. Zink, and D. L. Alkon. 1988. "Accelerating the convergence of the back-propagation method." *Biol. Cybern* 59 (4–5): 257–263. https://doi.org/10.1007/BF00332914.

Wang, C., Z. Jiang, L. Zhou, B. Dai, and Z. Song. 2019. "A functional group approach reveals important fish recruitments driven by flood pulses in floodplain ecosystem." *Ecol. Indic.* 99 (Sep): 130–139. https://doi.org/10.1016/j.ecolind.2018.12.024.

Whitfield, A. K., and M. Elliott. 2002. "Fishes as indicators of environmental and ecological changes within estuaries: A review of progress and some suggestions for the future." *J. Fish Biol.* 61 (Sep): 229–250. https://doi.org/10.1111/j.1095-8649.2002.tb01773.x.

Widrow, B., and M. E. Hoff. 1960. "Adaptive switching circuits." *IRE WESCON Conv. Rec.* 8 (4): 96–104.

Wild, T. B., P. M. Reed, D. P. Loucks, M. Mallen-Cooper, and E. D. Jensen. 2019. "Balancing hydropower development and ecological impacts in the mekong: Tradeoffs for Sambor mega dam." *J. Water Resour. Plann. Manage.* 145 (2): 05018019. https://doi.org/10.1061/(ASCE)WR.1943-5452.0001036.

Wong, T.-T. 2015. "Performance evaluation of classification algorithms by k-fold and leave-one-out cross validation." *Pattern Recognit.* 48 (9): 2839–2846. https://doi.org/10.1016/j.patcog.2015.03.009.

Yarnell, S. M., G. E. Petts, J. C. Schmidt, A. A. Whipple, E. E. Beller, and C. N. Dahm. 2015. "Functional flows in modified riverscapes: Hydrographs, habitats and opportunities." *Bioscience* 65 (10): 963–972. https://doi.org/10.1093/biosci/biv102.